Journal of Alloys and Compounds 495 (2010) 185–188

Contents lists available at ScienceDirect

Journal of Alloys and Compounds

journal homepage: www.elsevier.com/locate/jallcom

# Crystalline $MnV_2O_6$ nanobelts: Synthesis and electrochemical properties

Wenda Huang[a,b], Shaokang Gao[a,b], Xiaokun Ding[a], Lilong Jiang[a], Mingdeng Wei[a,c,*]

[a] Institute of New Energy Technology and Nano-Materials, Fuzhou University, Fuzhou, Fujian 350002, China
[b] College of Chemistry and Chemical Engineering, Fuzhou University, Fuzhou, Fujian 350002, China
[c] National Engineering Research Center of Chemical Fertilizer Catalyst, Fuzhou University, Fuzhou, Fujian 350002, China

ARTICLE INFO

*Article history:*
Received 30 November 2009
Received in revised form 20 January 2010
Accepted 21 January 2010
Available online 1 February 2010

*Keywords:*
$MnV_2O_6$
Nanobelts
Synthesis
Lithium intercalation
Electrochemical behavior

ABSTRACT

$MnV_2O_6$ nanobelts have successfully been synthesized via a hydrothermal route. The obtained nanobelts are highly crystalline and their thickness is found to be ca. 20–30 nm. These nanobelts were first used as the anode materials in a rechargeable lithium-ion battery, which exhibits a very reversible discharge/charge capacity and excellent cycling stability even at a current density as high as 1 A $g^{-1}$. This might be attributed to the intrinsic characteristics of $MnV_2O_6$ nanobelts.



## 1. Introduction

Nowadays, lithium-ion batteries (LIB) have widely been applied as a powder supply for portable electronic devices, such as digital cameras, note computers, cell phones, and TV watches. With increasing the popularization of micro-electronic devices, more powerful LIB have been demanded. LIB is constituted of two intercalation compounds as electrode materials. One is a lithiated metal oxide as cathode and the other graphite anode. For the latter, the graphite provides a favorable low potential for the lithium-ion intercalation/deintercalation and a long cycle life. Unfortunately, it suffers from small capacity per unit weight (theoretical capacity of 372 mA h $g^{-1}$) or per unit volume due to its low density and its rate property is not enough for the anode materials of large-scale batteries in the near future. To overcome these problems, much effort has been devoted to find out alterative anode materials for replacing graphite anode. A large number of materials such as oxides [1,2], nitrides [3], and metals [4,5] have been widely investigated. Recently, vanadate $MnV_2O_6$ has generated a new interest as an anode material because of its crystal structure. According to reports [6–12], the anode made of $MnV_2O_6$ exhibited a reversible capacity of 600–900 mA h $g^{-1}$ at the current densities of ~70 mA $g^{-1}$, which is larger than that of graphite.

In recent years, one-dimensional (1D) nanomaterials such as $TiO_2$–B nanowire [13], $TiO_2$ nanotube [14], and $V_2O_5$ nanoribbon [15], have successfully been applied in LIB, and a large capacity was obtained. According to report by Sides et al. [16], 1D nanomaterials based electrode showed unique rate capabilities for lithium batteries, because the diffuse of lithium ions is restricted to the radius direction, and the distance of diffuse is significantly smaller than that of electrode composed of usual particles. This encourages us to investigate $MnV_2O_6$ nanobelts anode with a large capacity and excellent cycling stability at a high current density. To the best of our knowledge, however, investigation on the electrochemical properties of $MnV_2O_6$ nanobelts has not been reported. In this study, $MnV_2O_6$ nanobelts were synthesized via a simple hydrothermal route and used them as the anode materials for lithium-ion intercalation at a high current density. The results of electrochemical measurement indicate that the anode composed of $MnV_2O_6$ nanobelts exhibits a large reversible capacity and excellent cycling stability.

## 2. Experimental

### 2.1. Preparation of electrode materials

The synthesis of $MnV_2O_6$ nanobelts was performed by a simple hydrothermal process. At first, 1 mmol of commercial $V_2O_5$ powder was dispersed into 40 mL of $H_2O$, and was then transferred into a 50 mL Teflon-lined autoclave, which was then kept in an oven at 200 °C for 1 day. After the reaction, a yellow solution was obtained. Secondly, 1 mmol of $MnCl_2{\cdot}4H_2O$ was added to the above yellow solution, and was then transferred to autoclave again, and kept at 180 °C for 8 days. The product was washed and filtered for several times, and dried at room temperature.

* Corresponding author at: Institute of New Energy Technology and Nano-Materials, Fuzhou University, Industrail Road 523, Fuzhou, Fujian 350002, China.
*E-mail address:* wei-mingdeng@fzu.edu.cn (M. Wei).

0925-8388/$ – see front matter © 2010 Elsevier B.V. All rights reserved.
doi:10.1016/j.jallcom.2010.01.116

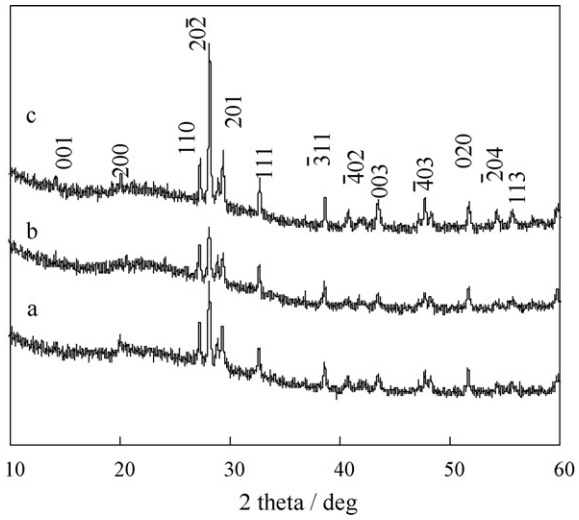


**Fig. 1.** XRD patterns of the products synthesized at 180 °C for different reaction times: (a) 2 days, (b) 4 days and (c) 8 days, respectively.

### 2.2. Characterizations of materials

X-ray powder diffraction (XRD) patterns were recorded using a diffractometer (Co Kα, PANalytical, X'Pert, data were convert into Cu Kα). Scanning electron microscope (SEM) and transmission electron microscopy (TEM) were taken on a Philip-XL30 instrument and a JEOL 2010 instrument, respectively.

### 2.3. Electrochemical measurements

For the electrochemical measurement, 60 wt% active materials were mixed and grounded with 10 wt% polyvinylidene fluoride (PVDF) powder as a binder and 30 wt% acetylene back carbon (AB) powder as the conductive assistant materials. The mixture was spread and pressed on Cu foil circular flakes as the working electrode (WE), and dried at 120 °C for 24 h under the vacuum conditions. Metallic lithium foils were used as the negative electrodes. The electrolyte was 1 M LiPF6 in a 1/1/1 (volume ratio) mixture of ethylene carbonate (EC), diethyl carbonate (DEC) and dimethyl carbonate (DMC). The separator was UP 3093 (Japan) micro-porous polypropylene membrane. The cells were assembled in a glove box filled with highly pure argon gas ($O_2$ and $H_2O$ levels <1 ppm), and charge/discharge tests were performed in the voltage range of 0.05–3 V ($Li^+/Li$) at current densities of 0.5 and 1 A $g^{-1}$ on a Land automatic batteries tester (Land CT 2001A, Wuhan, China).

## 3. Results and discussion

Fig. 1 shows X-ray patterns of the products synthesized at 180 °C for 2, 4 and 8 days. All the diffraction reflections can be indexed to a layered structure $MnV_2O_6$ (JCPDS 35-0139). The intensity of diffraction reflections increased with increasing reaction time, indicating that the crystalline of product was improved.

SEM images of the products synthesized at 180 °C for 2, 4 and 8 days are depicted in Fig. 2. As shown in Fig. 2a, the products are composed of a large quantity of the sheets. After the reaction time was increased to 4 days, the morphology of the product varied from sheet to belt, as depicted in Fig. 2b. When the reaction time was further increased to 8 days, nanobelts were formed. As shown in Fig. 2c, these nanobelts lie close to each other and their length is up to several tens of micrometers. Thus, it can be deduced that the sheets are an intermediate product in the formation process of nanobelts.

TEM measurements further confirmed the formation of a large number of nanobelts in the products, as shown in Fig. 3. The width of these nanobelts is found to be ca. 100–300 nm and the thickness is only 20–30 nm. These are in agreement with the results observed by SEM measurements. As shown in Fig. 3b, the high-magnification image clearly reveals highly crystalline nanobelts and the lattice fringe is 0.432 nm, corresponding to $d_{200}$ spacing in the XRD pattern of $MnV_2O_6$. A typical selected area electron diffraction (SAED) taken from a single nanobelt is presented in Fig. 3b (inset). These diffraction spots could be indexed onto $MnV_2O_6$ with a monoclinic structure.

In the present work, a simple method was developed to synthesize crystalline nanobelts. Based on the experiments results of XRD, SEM and TEM measurements, a possible model for the formation of nanobelts is described as follows: (i) $V_2O_5$ precursor was reacted with $H_2O$ to form $HVO_3$ solution; (ii) $HVO_3$ was reacted with $MnCl_4$ and the layered structure product $MnV_2O_6$ was obtained; (iii) $MnV_2O_6$ was gradually exfoliated to form sheets under the hydrothermal conditions; (iv) the sheets were splitted in order to release strong stress and lower the total energy, and then the nanobelts were formed. In fact, the synthesis of 1D nanomateri-

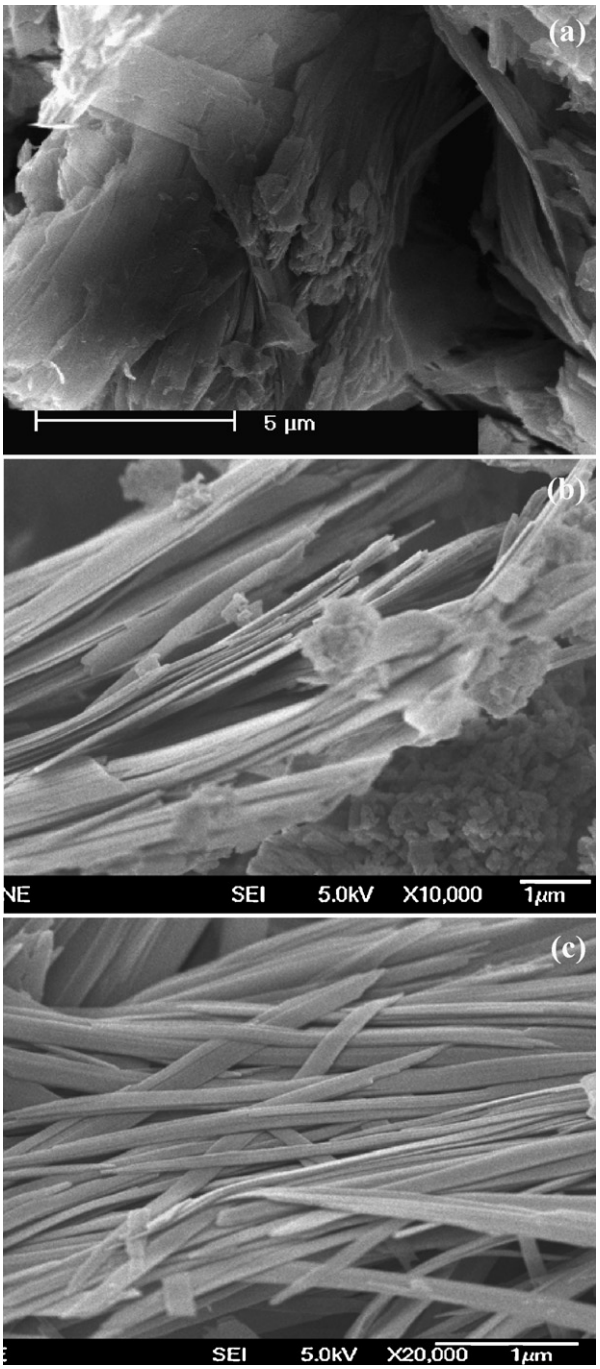


**Fig. 2.** SEM images of the products synthesized at 180 °C for (a) 2 days, (b) 4 days, and (c) 8 days, respectively.

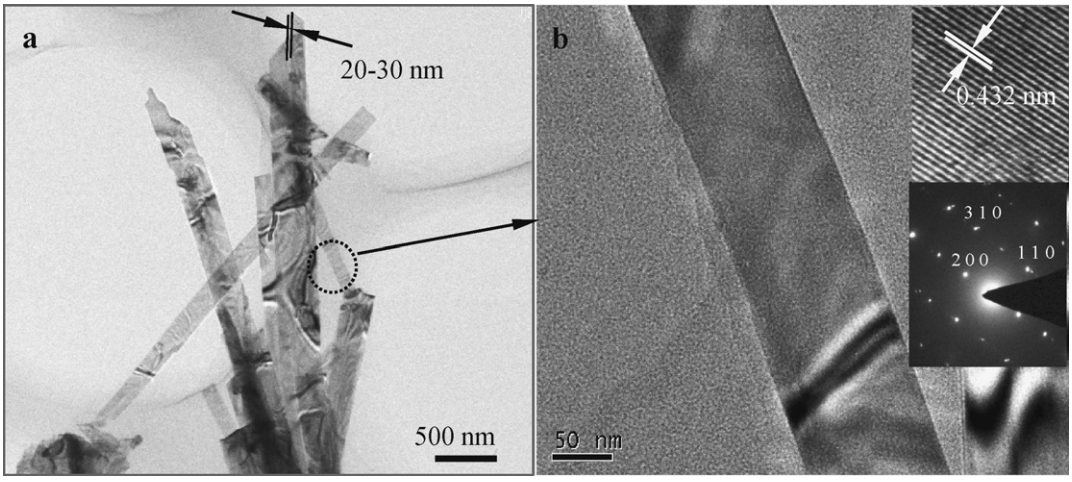


**Fig. 3.** TEM images of $MnV_2O_6$ nanobelts.

als using the layered compounds as the precursor has been widely reported [17,18].

The electrochemical performances of the $MnV_2O_6$ nanobelts were investigated, and the results are shown in Fig. 4. Fig. 4a shows the discharge–charge curves at a current density of 0.5 A $g^{-1}$, and a large irreversible discharge capacity of 1085 mA h $g^{-1}$ was observed. This can be attributed to the structure transformation to amorphous at the first cycle. It can be seen from Fig. 4b that the capacity trends to decrease in the initial cycling period, and then stopped decreasing and eventually reached a ceiling, indicating that the electrochemical properties of $MnV_2O_6$ nanobelts electrodes are very stable and the lithium-ion intercalation/deintercalation into/out of the electrodes is well reversible even at a current density as high as 1 A $g^{-1}$. A reversible capacity of 630 mA h $g^{-1}$ was obtained at a current density of 0.5 A $g^{-1}$ after 30 cycles, corresponding to $x = 6$ for $Li_xMnV_2O_6$. Even after the current density was increased to 1 A $g^{-1}$, a reversible capacity of 370 mA h $g^{-1}$ was also achieved, which is larger than that of graphite anode. This might be attributed to the intrinsic characteristics of electrode, where 1D nanostructured $MnV_2O_6$ nanobelts provide a short diffusion distance for Li ions intercalation/deintercalation into/out of the electrodes, as well as the Li ions adsorption on the surface of

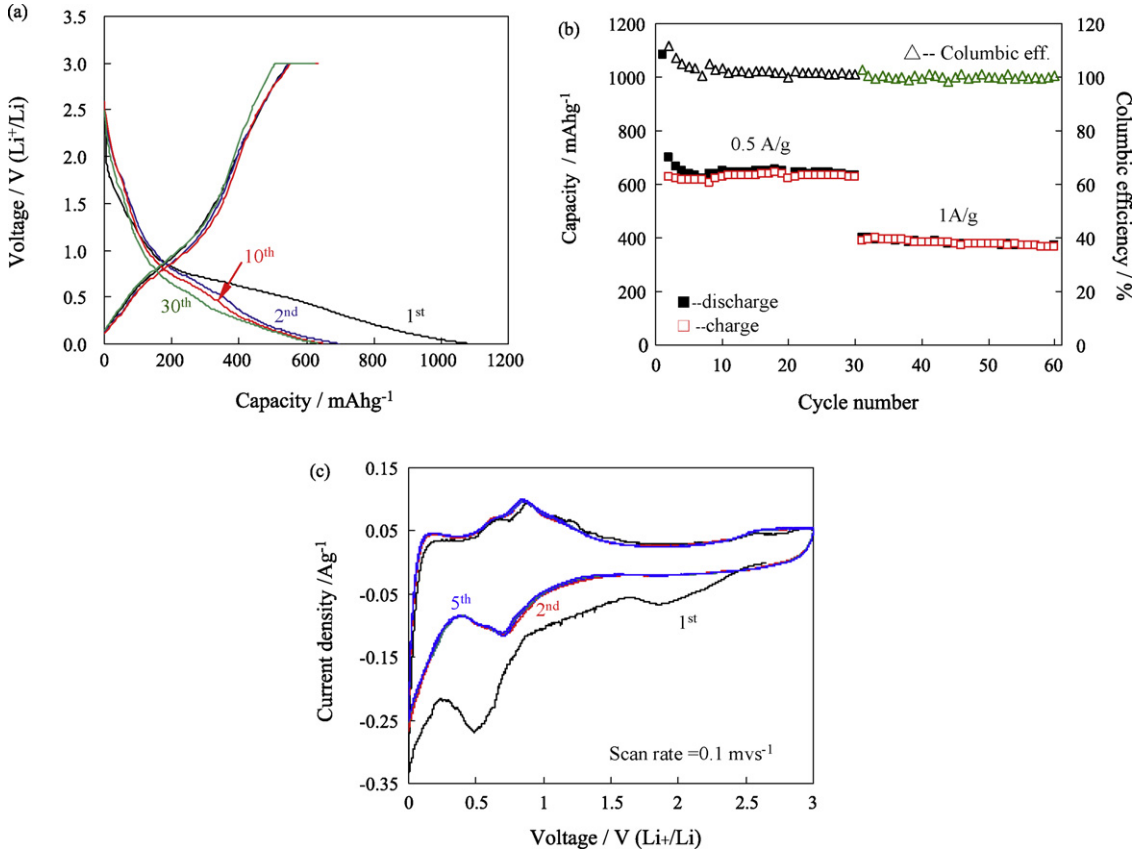


**Fig. 4.** The electrochemical behaviors of the electrode made of $MnV_2O_6$ nanobelts synthesize at 180 °C for 8 days. (a) charge–discharge profiles at a current density of 0.5 A $g^{-1}$, (b) cycle behaviors at current densities of 0.5 and 1 A $g^{-1}$, and (c) CV curves over the voltage range of 0.05–3 V.

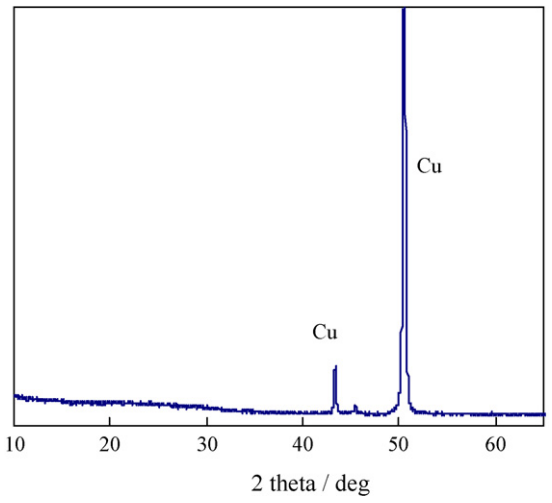


**Fig. 5.** XRD pattern of electrode made of $MnV_2O_6$ nanobelts after first cycle.

electrode, resulting in very excellent cycling stability. Although the initial capacity was as high as 900 mA h $g^{-1}$ for the electrode made of nanostructured $MnV_2O_6$, but the cycling stability is not satisfactory [11]. Using $MnV_2O_6$ particles as an electrode material, the capacity decreased with increasing cycling [7]. It also can be found that Coulombic efficiency (ratio of discharge capacity to charge capacity) for $MnV_2O_6$ nanobelts electrode being kept more than 100%, as shown in Fig. 4b. Fig. 4c shows the CV curves of $MnV_2O_6$ nanobelts at a scan rate of 0.1 mV $s^{-1}$. It can be found that the CV curves between the first cycle and the following cycles are different. This result might be attributed to the fact that the irreversible structured transformation has been taken place in the initial cycle. After the first cycle, the CV curves almost unchanged, indicating that lithium ions intercalation/deintercalation into/out of $MnV_2O_6$ nanobelts are well reversible.

Fig. 5 shows XRD pattern of electrode material made of $MnV_2O_6$ nanobelts after first cycle. Compared to XRD patterns in Fig. 1, it can be found that the main peaks of $MnV_2O_6$ disappeared, indicating that the crystal phase transformation occurred and amorphous phase was formed after the initial cycle. This is a reason that the initial capacity decreased severely after first cycle. The similar result was also observed by Wakihara and co-workers [7].

## 4. Conclusions

In conclusion, we have demonstrated a simple synthetic route for preparing $MnV_2O_6$ nanobelts. The synthesized nanobelts are highly crystalline and their thickness is found to be ca. 20–30 nm. These nanobelts were used as the electrode materials in a rechargeable lithium-ion battery, which displayed a large initial capacity of 1085 mA h $g^{-1}$. The electrode made of $MnV_2O_6$ nanobelts also exhibits a very reversible discharge/charge capacity and excellent cycling stability even at a current density as high as 1 A $g^{-1}$. These properties might be attributed to the intrinsic characteristics of $MnV_2O_6$ nanobelts. 1D structural nanobelts about 20–30 nm in width greatly reduced the diffusion distance of lithium ions and electrons in the solid state. On the other hand, the layered structure of $MnV_2O_6$ could provide a diffusion space for lithium-ion intercalation/deintercalation into/out of the electrodes, resulting in very good cycling stability.

## Acknowledgements

This study was financially supported by the National High Technology Research and Development Program (“863”) and Ministry of Education under Grant Nos. 2007AA05Z438 and 200803860004, Science and Technology Program from Fujian Province (Nos. 2008J0332 and 2007HZ0005-1) and the startup funds from Ministry of Education and Fuzhou University.

## References

[1] W.M. Zhang, X.L. Wu, J.S. Hu, Y.G. Guo, L.J. Wan, Adv. Funct. Mater. 18 (2008) 3941–3946.
[2] Z.H. Wen, Q. Wang, Q. Zhang, J.H. Li, Adv. Funct. Mater. 17 (2007) 2772–2778.
[3] T. Shodai, S. Okada, S.I. Tobishima, J.I. Yamaki, Solid State Ionics 86-88 (1996) 785–789.
[4] H. Kim, J. Cho, Chem. Mater. 20 (2008) 1679–1681.
[5] X.Y. Wang, Z.Y. Wen, Y. Liu, X.W. Wu, Electrochim. Acta 54 (2009) 4662–4667.
[6] Y. Piffard, F. Leroux, J.L. Mansot, M. Tournoux, J. Power Sources 68 (1997) 698–703.
[7] S. Kim, H. Ikuta, M. Wakihara, Solid State Ionics 139 (2001) 57–65.
[8] N. Ding, S.H. Liu, X.Y. Feng, H.T. Gao, X. Fang, J. Xu, W. Termel, I. Lieberwirth, C.H. Chen, Cryst. Growth Des. 9 (2009) 1723–1728.
[9] T. Morishita, H. Konno, Y. Izumi, M. Inagaki, Solid State Ionics 177 (2006) 1347–1353.
[10] D. Hara, J. Shirakawa, H. Ikuta, Y. Uchimoto, M. Wakihara, T. Miyanaga, I. Watanabe, J. Mater. Chem. 12 (2002) 3717–3722.
[11] M. Inagaki, T. Morishita, M. Hirano, V. Gupta, T. Nakajima, Solid State Ionics 156 (2003) 275–282.
[12] T. Morishita, K. Nomura, T. Inamasu, M. Inagaki, Solid State Ionics 176 (2005) 2235–2241.
[13] A.R. Armstrong, G. Armstrong, J. Canales, P.G. Bruce (Eds.), Angew. Chem. Int. 43 (2004) 2286–2288.
[14] K.X. Wang, M.D. Wei, M.A. Morris, H.S. Zhou, J.D. Holmes, Adv. Mater. 19 (2007) 3016–3020.
[15] C.K. Chan, H.L. Peng, R.D. Twesten, K. Jarausch, X. Zhang, Y. Cui, Nano Lett. 7 (2007) 490–495.
[16] C.R. Sides, N. Li, C.J. Patrissi, B. Scrosati, C.R. Martin, MRS Bull. 26 (2002) 604.
[17] M.D. Wei, Y. Konishi, H.S. Zhou, H. Sugihara, H. Arakawa, Solid State Commun. 133 (2005) 493–497.
[18] R.Q. Song, A.W. Xu, B. Deng, Y.P. Fang, J. Phys. Chem. B 109 (2005) 22758–22766.